

Electroplating: An Alternative for Producing Low Magnetic Loss Amorphous Alloys

R. Lacasse,^{1*} E. Potvin,¹ F. Allaire,² G. Houlachi,² J. Cave¹ and M. Trudeau¹

¹Hydro-Québec IREQ, Varennes, Québec, Canada

²Hydro-Québec LTE, Shawinigan, Québec, Canada

In recent years, Hydro-Québec's Research Institute has developed, through technological innovation, a program to improve energy efficiency in the generation, transmission and distribution of energy. Among the various projects, one was focused on the production of soft magnetic materials to improve the energy efficiency of distribution transformers. The aim of the project was to produce, by electrodeposition, free-standing foils or plates of amorphous Fe-P material having similar, or better, mechanical and low loss magnetic properties compared to iron-based amorphous alloys produced by rapid solidification. To meet this goal, an electroplating process was developed to produce a well-defined binary Fe-P amorphous alloy. The key electrochemical parameters, ancillary needs, critical monitoring and process controls were investigated. We succeeded in producing a fully amorphous soft magnetic material with very low power frequency losses and other advantageous properties such as a thickness range from 20 to 75 μm with a high production rate. Using thicker material, the production of stacked cores could be possible. In addition, electroplating offers the possibility of forming complex 2D shapes for rotating machines.

Keywords: Fe-P alloys, amorphous, soft magnetic properties, low magnetic losses, power distribution transformers

Introduction and background

Hydro-Québec as an electrical utility is continuously developing new methods and new technologies for improving the generation, transmission and distribution of electrical power. In December 2001, Hydro-Québec submitted its first Energy Efficiency Plan (EEP) to reduce consumption growth and carbon emissions. Hydro-Québec's Research Institute has developed a Technological Innovation Program to contribute to the development of more energy-efficient processes

and products. Among the various projects, one was focused on the production of soft magnetic materials to improve the energy efficiency of distribution transformers.

Amorphous or nanocrystalline soft magnetic materials that exhibit high saturation induction, high permeability, low coercivity and low core loss are desired for many alternating current (AC) applications. Rapid solidification technology development has facilitated the usage of metallic glasses. These alloys are usually made of about 20% metalloids such as silicon, phosphorus, boron or carbon and about 80% iron. Typical commercial thin ribbons have a thickness of 25 μm and a width of 210 mm.^{1,2} The transformer core loss of these alloys at an induction level of 1.4 tesla (T) are about 0.3 W/kg compared to 0.7 W/kg for best grade grain-oriented electrical steel, the commonly used material for core transformers.² Amorphous alloys can also be prepared by electrodeposition, vacuum deposition, sputtering and plasma spraying.

Electrodeposition of amorphous or nanocrystalline alloys based on iron group metals is one of the most important developments over recent decades in the field of soft magnetic thin films³ and nanotechnology applications.⁴ Iron-phosphorus alloys deserve special attention as cost effective soft magnetic materials for many applications. Electrodeposition has been extensively used to produce Fe-P alloy thin films, permitting control of the coating composition, microstructure, internal stress and magnetic properties,

*Corresponding author:

Dr. Robert Lacasse

Hydro-Québec

IREQ Research Institute

1800 boul. Lionel-Boulet

Varennes, Québec, Canada, J3X 1S1

Phone: (450) 652-8383

E-mail: lacasse.robert@ireq.ca

by using suitable plating conditions.⁵⁻¹¹ Electroplating has also been used to produce amorphous Fe-P coatings and electroforms for inductive devices such as amplifiers.¹²

The aim of the present work relates to the electrodeposition of thick free-standing foils or plates (20-75 μm) made of an amorphous Fe-P soft magnetic alloy, destined for large scale applications in electrical power equipment (transformers, rotating machines, etc.), that show high saturation induction, low coercive field and low power frequency losses.

Experimental

Electroplating conditions

Thick samples of Fe-P alloys were produced in a chloride bath. Table 1 shows the electroplating bath composition and the operating conditions used for three plating systems. The bath was an aqueous solution of $\text{FeCl}_2 \cdot 4\text{H}_2\text{O}$ and $\text{NaH}_2\text{PO}_2 \cdot \text{H}_2\text{O}$ at different concentration ranges depending on the plating system. Calcium chloride was added as a supporting electrolyte salt to improve solution conductivity for experiments conducted at 40-60°C. Some experiments were done by adding $\text{CuCl}_2 \cdot 2\text{H}_2\text{O}$ in the bath to electroplate a ternary Fe-P-Cu alloy. The pH of the solution ranged from 0.9 to 1.4 and was adjusted by the addition of hydrochloric acid. In all the experiments, a preliminary bubbling with nitrogen was performed in the aqueous plating solution and a small argon gas flow was maintained over the aqueous plating solution to prevent entry of oxygen.

At low temperatures (40-60°C), we used an electroplating system equipped with a rotating disk electrode (RDE). The cathode was a titanium disk 1.3 cm^2 in area and the anode was a dimensionally stable anode (DSA) 4 cm^2 in area. The rotation rate of the working electrode was mainly 900 rpm. The electroplating was performed using a DC current of 3-10 A/dm^2 .

For the LCD-HSV (Table 1) system at temperatures ranging from 40 to 70°C, a flow-through rectangular polypropylene cell with a large volume plating bath and equipped with parallel plates of 10 \times 15 cm was used. For the HCD-HSV (Table 1) system at temperatures ranging from 70 to 95°C, a flow-through rectangular Kynar (PVDF) cell system with a 40-liter volume plating bath and equipped with parallel plates of 2 \times 5 cm was used. The anode, made of DSA or graphite, had a surface area equal to that of the titanium cathode or was adjusted to a value allowing for control of any edge effect on the Fe-P deposit. The interelectrode gap between the working electrode and the anode was 5 mm. Electroplating was performed using DC current ranging from 4 to 110 A/dm^2 . The systems operated at a high concentration of the active species and at high plating solution velocities ranging from 100 to 350 cm/sec with a large ratio of bath to cell volume. The concentration of the hypophosphite and the pH at the cathode were closely controlled.

The titanium cathode was mechanically polished before use. The surface roughness was adjusted to be able to peel

Table 1
Composition of the bath and operating conditions

Chemicals and operating conditions	RDE cell	Parallel plate cell Low current density, high solution velocity LCD-HSV	Parallel plate cell High current density, high solution velocity HCD-HSV
$\text{FeCl}_2 \cdot 4\text{H}_2\text{O}$ (M)	1.0	1.0 - 1.5	1.0 - 1.5
$\text{NaH}_2\text{PO}_2 \cdot \text{H}_2\text{O}$ (M)	0.035 - 0.5	0.05 - 0.35	0.5 - 0.75
$\text{CaCl}_2 \cdot 2\text{H}_2\text{O}$ (M)	0.5	0.5	—
$\text{CuCl}_2 \cdot 2\text{H}_2\text{O}$ (mM)	0.0 - 0.3	0.0 - 0.02	—
Current density (A/dm^2)	1 - 5	4 - 30	30 - 110
Temperature ($^\circ\text{C}$)	40 - 60	40 - 70	70 - 95
pH	1.1 - 1.4	0.9 - 1.2	0.9 - 1.2
Rotation rate (rpm)	500 - 3000	—	—
Electrolyte velocity (cm/sec)	—	100 - 350	100 - 350
Cell or bath volume (L)	0.5	400	40
Cathode: material, dimension (cm^2)	Ti disk, 1.3	Ti plates, 150	Ti plates, 10
Anode	DSA	DSA or graphite	DSA or graphite
Reference electrode	SCE	—	—

off the Fe-P foil, while keeping adhesion sufficiently high to avoid the detachment of the deposit during the process.

Hydrogen removal, annealing and Fe-P characterization

In the present work, production of Fe-P plates comprises one or more additional steps in order to improve their magnetic properties. First, a thermal treatment was performed at 120°C for 10 min for hydrogen removal after the amorphous foil was peeled from the working electrode. Second, a further annealing treatment from 200 to 325°C of the amorphous Fe-P foil was performed for stress relief.

The XRD characterization was made by using a Bruker D8 Advance x-ray diffractometer with CuK α radiation. Scattering angles (2θ) from 30° to 60° were measured and the amorphousness analysis was based on the presence or absence of α -Fe diffraction peaks attributed to large crystals. The composition of the alloys was determined by the inductively-coupled plasma emission spectral analysis (Perkin-Elmer® Optima 4300 DV), using appropriate standards and after dissolution of the sample in 5% nitric acid.

The thermal stability of the alloys as a function of temperature was determined by differential scanning calorimetry (DSC) using a Perkin-Elmer DSC-7 with a temperature scanning rate ranging from 5 to 20 K/min.

The magnetic measurements fall into three categories. First, using an ADE EV7 vibrating sample magnetometer (VSM), the measurements of the basic physical materials properties such as the saturation magnetization and the corresponding coercive field H_c in quasi-static conditions, were performed. Second, using an in-house integrating magnetometer, the performances of many similar samples (disk or 1 x 4 cm samples) were compared, at power frequencies (around 60-64 Hz) for a sine wave-applied magnetic field (up to around 8000 A/m), and by obtaining the losses and corresponding induction and an estimate for H_c . Third, an in-house integrator for a no-load transformer configuration similar to a four-leg Epstein frame, with the primary and secondary windings wound tightly onto each leg, was used. The measurements were carried out by integrating the pick-up voltage of the secondary of the sample and of a calibrated air core transformer in series with the sample in order to obtain waveforms for the magnetic induction and applied field strength respectively. A feedback system ensured as near as possible a sine wave induction in the sample. The hysteresis (B-H) loops were then integrated to obtain the losses. To allow for a small overlap of each leg at the corners of the sample, the weight used to obtain the losses was reduced to that calculated using the path length multiplied by the cross section (which was previously calculated from the total weight divided by the density and by the total length). The power frequency losses and the corresponding value of H_c from the analysis of individual hysteresis (B-H) loops were then obtained. Measurements were confirmed for consistency using a commercial hysteresis measurement apparatus (Walker AMH20).

Saturation induction (B_s). This magnetic parameter was measured using a commercial VSM or from the transformer

measurement (in-house integrator and Walker AMH20).

Low coercive field (H_c). This parameter was quantified using a VSM (physical measurement) and an in-house integrating magnetometer (comparative measurement) and a transformer configuration (to obtain H_c as a function of peak induction).

Power frequency losses (W_{60} , hysteresis, eddy current and anomalous losses). This parameter was quantified as a function of peak induction using the in-house transformer configuration and compared between samples using the in-house magnetometer measurement for inductions near to saturation.

Electrical resistivity (ρ_{dc}). This physical parameter was measured with a four-contact direct current method on short samples, with gauge length of about 1 cm (HP current supply, Keithly® nanovoltmeter).

Results and discussion

Fe-P alloy composition and structure

A number of foils were prepared with a rotating disk electrode cell at temperatures ranging from 40 to 60°C to determine the influence of the phosphorus content on the microstructure and on the magnetic properties of the Fe-P foil. Figure 1 shows the relation between the at% P in foils of 50 μ m thickness versus the concentration of the phosphorus precursor in the plating bath and the cathodic coulombic efficiency (CE). The phosphorus content, ranging from 12-16 at% in the foil, increased linearly with the phosphorus content in solution and was inversely related to the cathodic CE. In this range, a preferential deposition of phosphorus was observed. At phosphorus contents higher than 16 at%, the CE drops rapidly and is associated with a greater difficulty in adding phosphorus in the alloy.

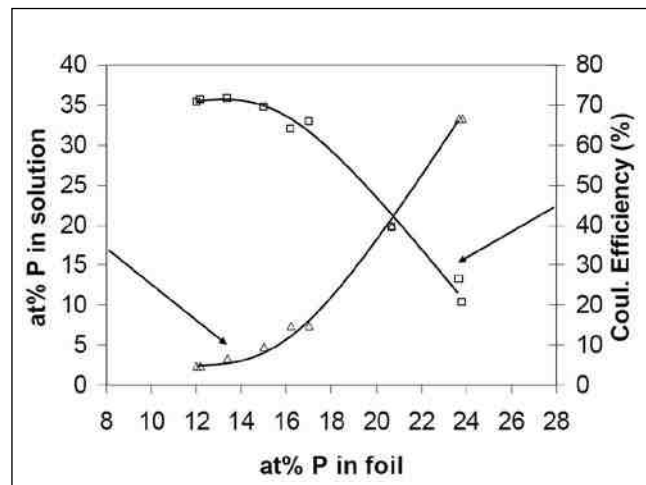


Figure 1 - Relation between the phosphorus content in Fe-P foils of 50 μ m thickness with the concentration of hypophosphite in the aqueous plating bath and the coulombic efficiency: 1.0M FeCl₂, 0.025-0.5M NaH₂PO₂, 0.5M CaCl₂, 40°C, 4.0 A/dm².

It is well known that Fe-P produced by electrodeposition gradually changes from a microcrystalline to an amorphous structure by increasing the phosphorus content in the alloys.¹³⁻¹⁴ For RDE-electrodeposited samples in the present work, the amorphous structure as shown by x-ray diffraction was obtained with an at% P higher than 15% (Fig. 2). The x-ray diffraction pattern at 17 at% P revealed no crystalline peaks except for the small region surrounding the foil (due to an edge effect).

From the analysis of Fig. 1 and the XRD characterization, the transition between the two electrodeposition regimes seems to correspond to the change from microcrystalline to amorphous structure.

To determine the range of annealing temperatures required to avoid the crystallization of the amorphous matrix, the thermal stability of the present amorphous Fe-P samples was studied by differential scanning calorimetry (DSC). Figure 3 shows that the amorphous Fe-P foil exhibits only one strong exothermic peak at around 410°C. A short low-temperature thermal treatment (from 200 to 325°C) of the amorphous Fe-P foils was performed with and without the presence of an applied magnetic field (Fig. 3 insert). The insert shows a decrease of the coercive field H_c by 64% as the temperature is increased from 25°C to around 300°C. This drastic change in H_c occurs at a temperature below the crystallization temperature. After crystallization, the material loses its soft magnetic behavior. The treatment time and temperature were optimized to obtain the lowest coercive field values. The treatment time was around 10 sec at 300°C, to around one hour at 200°C. For instance, it would be about 15 min around 265°C. The mechanism responsible for the decrease of H_c was probably a stress relief of the structure.¹¹

Before focusing on the electroplating of a binary Fe-P alloy, some attempts were made at electroplating a ternary Fe-P-Cu alloy. The DSC trace of the amorphous $Fe_{85}P_{14}Cu_1$ foil shows the presence of two exothermic peaks at around 366 and 383°C. The electroplating of the ternary alloy was postponed because of the difficulty of controlling the copper content, since its deposition is diffusion-controlled.

The samples considered in Figs. 1 and 2, annealed for 30 min at 250°C under a magnetic field, were used to determine the phosphorus content range in the foils necessary to obtain the lowest coercive field (H_c magnetometer measurement) while maintaining a high saturation induction. Figure 4 shows a minimum H_c value near 17 at% P, corresponding to the amorphous structure of the alloy (as seen in Fig. 2). These results reveal that a good compromise for the phosphorus content can be found that ensures a low H_c value with a good coulombic efficiency while maintaining a high saturation induction (which depends on keeping the iron content as high as possible). At different bath temperatures, this optimum value will change in accordance with variation in the H_c and the coulombic efficiency family of curves.

High solution velocity and high deposition rate

The performance of electrochemical processes depends on several factors, such as charge transfer and electrode kinetics, and fluid dynamic conditions, which are the most

critical as they control the mass and heat transport. The productivity of the RDE cell is poor due to operation at low current densities and with a cell design resulting in a low space-time yield. Thus, the technical challenge facing our work was to design an electrochemical cell that allowed for producing a cathode deposit of homogeneous phosphorus content with high coulombic efficiency while maintaining a low coercive field. The cell design in our work consisted of a flow-through rectangular cell containing one cathode and one anode both 10 × 15 cm (40-70°C) or 2 × 5 cm (70-95°C). The entry and exit flow channel lengths of the cell were adjusted to attain fully developed turbulent electrolyte flow. This cell design, operating at a high solution velocity of up to 350 cm/sec and high current densities, allowed good uniformity of electroactive species concentration at the electrode surface while minimizing local pH variation and other concentration changes due to electrode reactions.

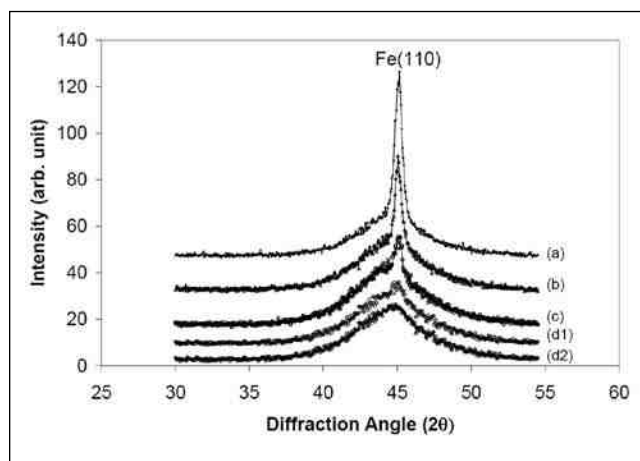


Figure 2 - X-ray diffraction patterns of Fe-P foils of 50 μm thickness as-deposited with different phosphorus contents: (a) 12 at% P, (b) 13.5 at% P, (c) 15 at% P, (d) 17 at% P with the edge effect and (d₂) 17 at% P without the edge effect.

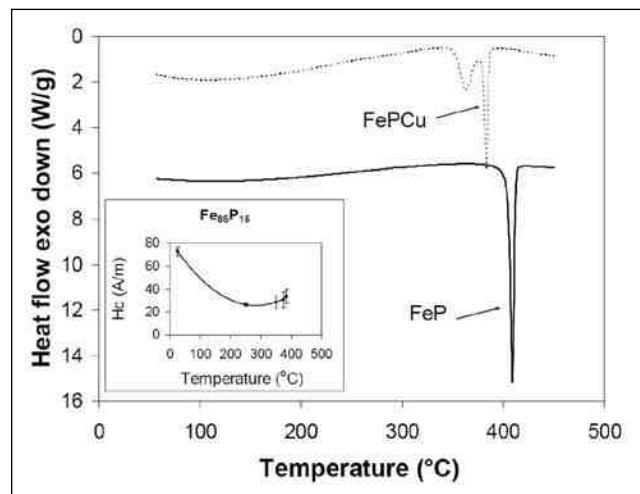


Figure 3 - Differential scanning calorimetry traces obtained with an amorphous Fe-P foil compared with an amorphous Fe-P-Cu foil (scanning rate 20 K/min.); (Insert: H_c vs. temperature for Fe-P alloy; VSM measurements ±10%).

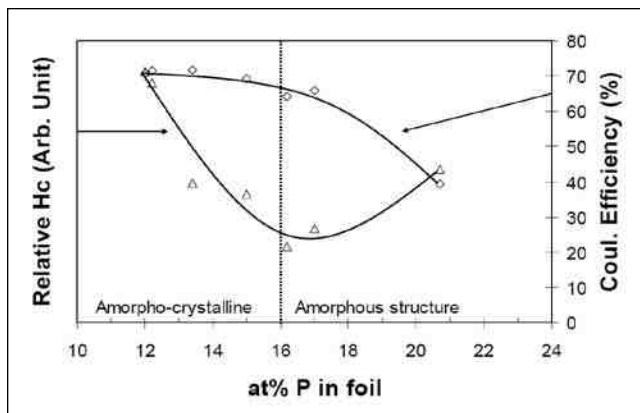


Figure 4 - Relationship between the phosphorus content in Fe-P foils of 50 μm thickness with the coulombic efficiency and the relative coercive field H_c (magnetometer measurement) after annealing for 30 min at 250°C (electroplating conditions as in Fig. 1).

Fe-P electrodeposition: Low current density and high solution velocity (LCD-HSV)

The development work with the flow-through rectangular cell started with the same bath composition and operating conditions except for the fluid dynamic conditions. For instance, sample foils of 10 \times 15 cm were produced at a low current density of 4.0 A/dm² at 60°C with a solution velocity of 300 cm/sec with an inter-electrode gap of 5 mm. The plating solution had the following composition: 1.0M FeCl₂·4H₂O, 0.1M NaH₂PO₂·H₂O, 0.02mM CuCl₂·2H₂O and 0.5M CaCl₂·2H₂O. The pH was 1.15. An analysis of one foil gave a composition Fe_{81.8}-P_{17.8}-Cu_{0.4}. The coulombic efficiency was 53% for a thickness of 70 μm . The homogeneity of the phosphorus content across the thickness was 18.4 \pm 0.24 at% P and the SEM micrographs show low porosity. With these conditions, easy peel off and manipulable 30-70 μm thick samples were obtained.

Although the high solution velocity Fe-P deposits containing 17-20 at% P had acceptable characteristics for temperatures ranging from 40 to 70°C, increasing the current density for these bath conditions led to highly stressed deposits. This was explained by the formation of amorpho-crystalline deposits because of the difficulty of further increasing the phosphorus content in this set of conditions.

Fe-P electrodeposition: High current density and high solution velocity (HCD-HSV)

For high space-time yield production of Fe-P deposits containing 17-20 at% P, the concentration ratio P/Fe in solution was increased, and the phosphorus content in the foils was investigated as a function of bath temperature, solution velocity and current density. Sample foils of 2 \times 5 cm were produced at high current densities as described in Table 1. Figure 5 shows the variation of the phosphorus content in the foil for different solution velocities at 70°C and at a current density of 20 A/dm². For a velocity increase from 110 cm/sec to 160 cm/sec, the phosphorus content increased by approximately 1.0 at% in the foil.

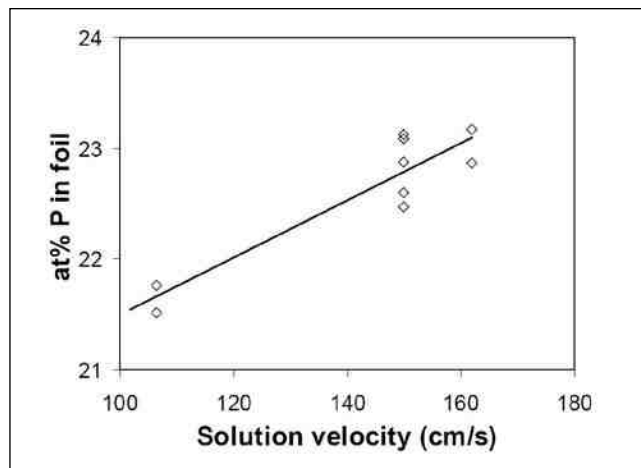


Figure 5 - Effect of solution velocity on the phosphorus content of the Fe-P foils; 1.0M FeCl₂, 0.5M NaH₂PO₂, 70°C, 20 A/dm² with the HCD-HSV system.

Figure 6 shows the variation of phosphorus content in the foils at different current densities for three different temperatures. For the same electrolyte conditions and solution velocity, increasing the temperature from 70°C to 95°C permitted a three-fold increase in the current density while keeping the alloy composition in the range of 17-20 at% P. At a temperature of 95°C, easy peel off, easy handling, low porosity, low stress foils of 50-75 μm in thickness were obtained at current densities as high as 100 A/dm² with coulombic efficiencies of 64 \pm 4%.

Amorphous characterization properties of Fe-P foils

Specimen foils were produced under both LCD-HSV and HCD-HSV conditions and annealed to minimize H_c . Figure 7 shows the x-ray diffraction patterns obtained as-deposited and at different temperatures: 275, 288 and 425°C. The x-ray diffraction patterns reveal an amorphous structure for the as-deposited and annealed samples at 288°C. Annealing a foil at temperatures higher than the exothermic peak

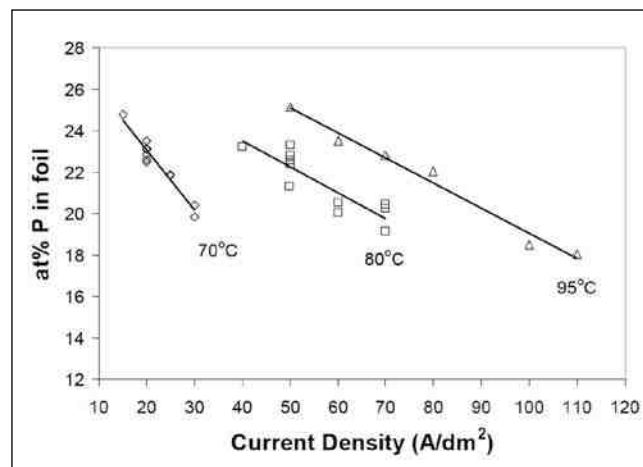


Figure 6 - Effect of temperature and current density on the phosphorus content of the Fe-P foils; 1.0M FeCl₂, 0.5M NaH₂PO₂, solution velocity=180 cm/sec with the HCD-HSV system.

around 400°C induced a transformation from the amorphous phase to a crystalline BCC Fe and Fe₃P structure. Table 2 shows the optimization of the annealing temperature for minimizing the coercive field.

Fe-P power frequency losses

LCD-HSV specimens 1 × 4 cm were cut from a 10 × 15 cm foil and were annealed for 15 min at 265°C under an argon atmosphere and in a magnetic field produced by permanent magnets that completed a magnetic circuit with the samples.

Figure 8 shows the power frequency losses (W_{60}), in a reduced size Epstein frame configuration, with corresponding values of coercive field (H_c) as a function of the peak induction B_{max} . The actual losses presented in the figure are estimated to be about 5% higher due to the overlap section of the sample segments. The power frequency loss (W_{60}) at peak induction of 1.35 T was 0.39-0.41 W/kg. The coercive force (H_c) after an induction of 1.35 T was 13 A/m ± 5%. The saturation induction was 1.5 T ± 5%. The electrical resistivity (ρ_{dc}) of the foil was 165 ± 15% $\mu\Omega\cdot\text{cm}$.

HCD-HSV specimens 1 × 4 cm were cut from several different 2 × 5 cm sample foils and annealed as previously described to construct another Epstein transformer configuration sample.

Figure 9 shows the power frequency losses (W_{60}) and corresponding values of the coercive field (H_c) as a function of the peak induction B_{max} . The actual losses presented in the figure are estimated to be about 10% higher due to the overlap section of the sample segments. The power frequency loss (W_{60}) at peak induction of 1.35 T was 0.395-0.434 W/kg. The coercive force (H_c) after an induction of 1.35 T was 9.9 A/m ± 5%. The saturation induction was 1.4 T ± 5%. The average electrical resistivity (ρ_{dc}) of these foils was 142 ± 15% $\mu\Omega\cdot\text{cm}$.

These power frequency results shows that we have succeeded in producing low loss thick amorphous Fe-P foils by electrodeposition at low and at high deposition rates.

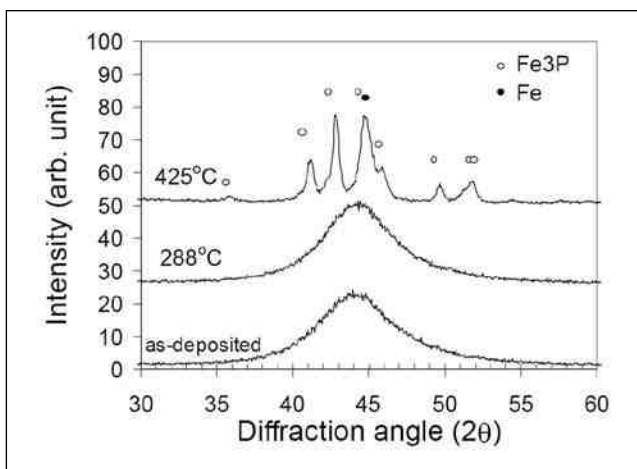


Figure 7 - X-ray diffraction patterns of 50 μm thick Fe-P foils. An as-deposited sample is compared with annealed ones below (288°C) and above (425°C) the DSC transformation peak (Conditions: HCD-HSV deposition).

Table 2

Effect of annealing temperature on the variation of the coercive field (VSM measurements ± 10%)

Annealing Temperature (°C)	LCD-HSV Fe ₈₂ -P _{17.5} -Cu _{0.5} H _c (A/m)	HCD-HSV Fe _{82.5} -P _{17.5} H _c (A/m)
As-deposited	26	51
275	20	---
288	15	13
425	3700	> 3000

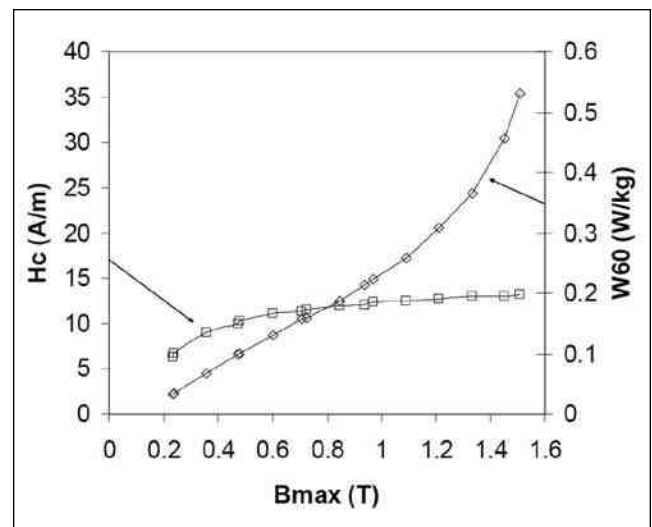


Figure 8 - Power frequency losses (W_{60}) and corresponding values of coercive field (H_c) as a function of the peak induction B_{max} (Conditions: LCD-HSV deposition).

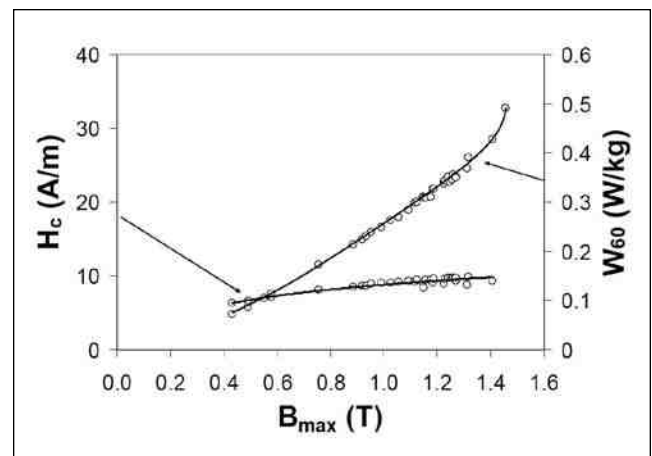


Figure 9 - Power frequency losses (W_{60}) and corresponding values of coercive field (H_c) as a function of the peak induction B_{max} (Conditions: HCD-HSV deposition).

Conclusions

The aim of the present work relates to the electrodeposition of thick foils or plates (20-75 μm) of an amorphous Fe-P soft magnetic alloy, destined for large scale applications in electrical power equipment (transformers, rotating machines, etc.), that show high saturation induction, low coercive field and low power frequency losses.

The conditions for producing good amorphous Fe-P material have been systematically studied. In particular, a high current density, high solution velocity (HCD-HSV) process has been identified which could lead to a competitive and economical industrial process based on electrodeposition.

The 60 Hz AC loss properties are very encouraging at around 0.4 W/kg at 1.35 T maximum induction. This places the losses between those of metallic glasses and grain-oriented electrical steels.

Further advantages of these electrodeposited materials, for developing power applications, are that much greater thicknesses than metallic glasses can be achieved and that complex 2D shapes for rotating machines could be envisioned. Further evaluation of technical as well as economic aspects and a pilot production demonstration will follow.

Acknowledgements

This work was sponsored by Hydro-Québec Technological Innovation Program. The authors gratefully acknowledge helpful discussion with Dr. Ashok Vijh. We also thank F. Brochu, M. Provencher, R. Rioux, R. Veillette, J. Beaudry, I. Montplaisir and P. Noël for their technical assistance.

References

1. G.E. Fish, *Proc. IEEE*, **78** (6), 947 (1990).
2. N. DeCristofaro, *MRS Bulletin*, **23** (5), 50 (1998).
3. E.I. Cooper, *et al.*, *IBM J. Res. & Dev.*, **49** (1), 103 (2005).
4. G. Palumbo, *et al.*, *Plating & Surface Finishing*, **90** (2), 36 (2003).
5. A. Brenner, *Electrodeposition of Alloys: Principles and Practice*, Vol. 2, Academic Press, New York, NY, 1963.
6. J. Logan & M. Yung, *J. Non-Crystalline Solids*, **21** (1), 151 (1976).
7. S. Uedaira, U.S. Patent 4,101,389 (1978).
8. St. Vitkova, M. Kjachukova & G. Raichevski, *J. Appl. Electrochem.*, **18** (5), 673 (1988).
9. T. Osaka, *et al.*, *J. Magnetism Soc. Japan*, **18**, 187 (1994).
10. K. Kamei & Y. Maehara, *Mat. Sc. and Eng. A*, **181/182**, 906 (1994).
11. K. Kamei & Y. Maehara, *J. Appl. Electrochem.*, **26** (5), 529 (1996).
12. R.L. Gamblin, U.S. Patent 4,533,441 (1985).
13. G. Dietz, *et al.*, *Z. Phys. B: Condensed Matter*, **81** (2), 223 (1990).
14. F. Wang, K. Itoh & T. Watanabe, *Mat. Trans.*, **44** (1), 127 (2003).

About the authors

Dr. Robert Lacasse is a Research Scientist at the Hydro-Québec Research Institute in Varennes, which he joined in 1995, with expertise in lithium batteries, materials innovation and diagnostic methods such as thermography and electrochemical noise. In recent years, Dr. Lacasse's interest has been focused on the electrodeposition of nanocrystalline and/or amorphous materials for power applications with particular emphasis on soft magnetic materials. He received his M.S. from Sherbrooke University in Québec, Canada. He then continued his education in France at the Burgundy University in collaboration with Sherbrooke University and earned a Ph.D. in Electrochemistry in 1993. He is the author or co-author of 12 peer reviewed papers.



Dr. Estelle Potvin is a Research Scientist at the Hydro-Québec Research Institute in Varennes where she has been involved in applied electrochemistry since 1990. Her professional experience includes corrosion and development of materials for water electrolysis and lithium-metal-polymer batteries, and more recently in the development of amorphous ferromagnetic alloys by electrodeposition for AC power applications. She is currently working on the development of materials for industrial wastewater treatment. She has to her credit 11 peer reviewed papers and five patents as author or co-author. She obtained her Ph.D. degree from Sherbrooke University in 1990 in electrochemistry.

Dr. François Allaire is a Research Scientist with Hydro-Québec at the LTE laboratory in Shawinigan (since 1992). He previously worked for the Industrial Materials Institute. During those years, he contributed to the development of processes in plasma powder production, lithium metal polymers and Li-ion battery components. He also worked on electrochemical projects on Zn, Cu, Au and Fe-P alloy deposition. He holds a Ph.D. degree in Chemistry from the Université de Montréal.



Georges Houlachi is a Research Scientist at the Hydro-Québec Research Institute at the LTE laboratory in Shawinigan. Previously, he has worked at the Noranda Technology Centre in Montreal as a Principal Scientist with expertise in hydro- and electrometallurgy. Currently, he has contributed to the development and implementation of electrochemical processes in copper and zinc refining. He has been involved in projects on Au, Ti, Al and Fe-P alloy deposition. He is the author of 33 papers and 14 patents. He is a member of the

CIM society, Hydrometallurgy section committee and the Green Mining executive committee at CANMET. He holds a B.Sc. in Chemistry from the American University in Lebanon followed by graduate studies at Ecole Polytechnique in Montreal.

Dr. Julian Cave is a Research Scientist at the Research Institute of Hydro-Québec, where he has been investigating the use of superconductors in power networks for the last 20 years. These studies have included fault current limiters, SMES, magnetic bearings and more recently superconducting rotating machines. A more recent interest has been in the characterization of amorphous ferromagnetic alloys destined for power applications such as transformers. He has served as a DOE Peer Review panel member for Superconductivity for Electric Systems. He previously worked in France for Alstom-Alcatel Recherche on ultra-fine multi-filamentary superconducting wires and before that was a Fellow of Magdalene College, Cambridge, UK. He obtained his B.Sc. degree from the University of Bristol in Physics and Maths in 1974 and his Ph.D. degree from the University of Cambridge in 1979 for studies on complex flux configurations in type II superconductors.



Michel L. Trudeau has been involved in the understanding and physical characterization of metastable and nanostructured materials for nearly 30 years. One of his main interests is the relation between the structural and physical properties of metastable and nanostructured materials used for energy efficiency or applications. He is also in charge of the Hydro-Québec Materials Characterization Laboratory. He is the author or co-author of 123 peer reviewed papers and has written four book chapters and edited one conference proceeding. He has co-chaired seven international meetings related to nanostructured materials. In 1991, he co-chaired the first symposium on Nanocrystalline Solids at the March APS meeting, well before high interest in nanostructured materials developed. In 2008 he was elected as a Fellow of the American Physical Society for his work on nanostructured materials.

NASF Events



NASF Management Conference February 27-March 3, 2011 Point Hilton Tapatio Cliffs Resort Phoenix, Arizona

We hope that you'll find the 2011 program to be just the right mix of business and pleasure. From the 18-hole championship golf course, hiking in the Sonoran Desert to the three-acre oasis of swimming pools, the resort offers many recreational opportunities. The business meetings will focus on issues that face our industry. You'll hear from your peers on various topics that directly relate to your business and you'll have the opportunity to participate in panel discussions. [Click here for more information.](#)



NASF Washington Forum April 12-15, 2011 Arlington, VA Ritz-Carlton Pentagon City Hotel

Don't miss the opportunity to be in the nation's capitol next spring for the 2011 NASF Washington Forum.

This event gives attendees the latest updates and insights on key policy issues and trends impacting the finishing business today. [Click here for more information.](#)



SUR/FIN 2011 June 13-15, 2011 Rosemont, IL Donald E. Stephens Convention Center

SUR/FIN is the only show in North America dedicated to surface finishing. Come to the industry's trade show and visit over 200 vendor booths and learn more about your industry through the expansive technical program. [Click here for more information.](#)